Molecular Phylogenetic Analysis of the Amiota taurusata Species Group within the Chinese Species, with Descriptions of Two New Species

Authors: Shao, Zhen-fang, Li, Tong, Jiang, Jian-jun, Lu, Jin-ming, and Chen, Hong-wei

Journal of Insect Science
www.insectsscience.org

Molecular phylogenetic analysis of the *Amiota taurusata* species group within the Chinese species, with descriptions of two new species

Zhen-fang Shao[1a], Tong Li[2b], Jian-jun Jiang[1c], Jin-ming Lu[1d], and Hong-wei Chen[1e]*

[1]Department of Entomology, South China Agricultural University, Tianhe, Guangzhou, Guangdong, 510642, China
[2]Institute of Plant Protection, Henan Academy of Agricultural Science, Jinshui, Zhengzhou, Henan, 450002, China

Abstract

The relationships among six species of the *Amiota taurusata* Takada, Beppu, & Toda (Diptera: Drosophilidae) species group were investigated based on DNA sequence data of the mitochondrial NADH dehydrogenase subunit 2 (*ND2*) gene, using three species of the genus *Amiota* as outgroups. A mitochondrial gene, cytochrome *c* oxidase I (*COI*), can be used to discriminate between species of the *taurusata* group. Two new species are described from South China: *A. protuberantis* Shao et Chen, **sp. nov.** and *A. shennongi* Shao et Chen, **sp. nov.** A key to all the species of the *taurusata* group based on morphological characters is provided.

> **Cite this paper as:**
> Shao Z-f, Li T, Jiang J-j, Lu J-m, Chen H-w. 2014. Molecular phylogenetic analysis of the *Amiota taurusata* species group within the Chinese species, with descriptions of two new species. *Journal of Insect Science* 14:33. Available online: http://www.insectsscience.org/14.33

Introduction

The *Amiota taurusata* Takada, Beppu, & Toda (Diptera: Drosophilidae) species group was established by Chen and Toda (2001) based on a phylogenetic analysis using 31 adult male morphological characters. Until now, eight species have been reported in this group from East Asia (Chen and Toda 2001; Chen et al. 2004, 2005; Cao et al. 2008): *A. aquilotaurusata* Takada et al., 1979, *A. asymmetrica* Chen et Takamori, 2005; *A. femorata* Chen et Takamori, 2005, *A. sacculipes* Máca et Lin, 1993, *A. spinifemora* Li et Chen, 2008, *A. taurusata* Takada et al., 1979, *A. vulnerabla* Chen et Zhang, 2004, and *A. yixiangensis* Chen et Takamori, 2005. Chen and Toda (2001) regarded the *taurusata* group as monophyletic on the basis of the hind femur basoventrally with a small, lobe-like flap (ch. 1; Figure 2D in Chen and Toda 2001); hind tibia apicodorsally much extended flap (ch. 2; Figure 2D in Chen and Toda 2001); hind first tarsomere dorsally expanded (ch. 3; Figure 2D in Chen and Toda 2001); fourth tergite laterally broadened and protruded more than others (ch. 4; Figure 1B in Chen and Toda 2001). However, Chen et al.

(2004, 2005) and Cao et al. (2008) found that the ch. 2 and ch. 3 are usually absent in some species; these two characters have been eliminated from the diagnosis criteria of the *taurusata* group.

Recently, a molecular approach was used to uncover the relationship among the species in *Stegana* (Li et al. 2010; Lu et al. 2011a, b), *Phortica* (He et al. 2009b; Cao et al. 2011), and *Paraleucophenga* (Zhao et al. 2009), which are from genera of the subfamily Steganinae. However, few related studies have been carried out in the genus *Amiota*. Chen and Toda's (2001) phylogenetic analysis of the subgenus *Amiota* (currently the genus *Amiota*) included the three species of this group mentioned above, the *taurusata* group, which is closely related to the *apodemata*, the *nagatai*, and the *sinuata* groups, but the relationships within this group were not resolved at all. In the present study, two new species of the *taurusata* group from China are described, and the relationships among the four known and two new species were investigated based on the DNA sequences of the mitochondrial NADH dehydrogenase subunit 2 (*ND2*) gene. Barcoding information on the mitochondrial cytochrome *c* oxidase I (*COI*) genes of most of the species is provided.

Figure 1. *Amiota protuberantis* Shao et Chen, **sp. nov.** ♂: (A) Epandrium (epand) and circus (cerc), lateral view; (B) surstylus (sur) and tenth sternite (st 10), ventral view; (C) hypandrium and gonopod, ventral view; (D) paramere, aedeagus, and aedeagal apodeme, lateral view. Scale bars: 0.1 mm. High quality figures are available online.

Materials and Methods

Materials
All materials were collected from tree trunks or around human eyes and preserved in 75% ethanol. A small piece of tissue was removed from the fly abdomen and used for the DNA extraction. The body and terminalia were dried and deposited in the Department of Entomology, South China Agricultural University, Guangzhou, China (SCAU). The definitions of measurements, indices, and abbreviations follow Zhang and Toda (1992)
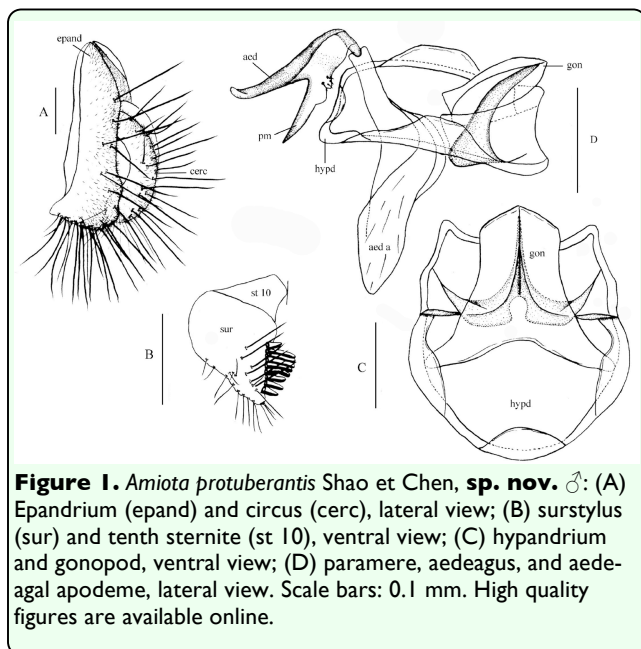
and Chen and Toda (2001).

The information on the samples used in the molecular phylogenetic analyses is given in Table 1. Six species of the *taurusata* group were employed in the molecular phylogenetic analysis, and three *Amiota* species of the genus *Amiota* from the *apodemata*, *nagatai*, and *sinuata* groups were used as outgroups.

Abbreviations

4c, third costal section between R2+3 and R4+5/M1 between r-m and dm-cu; **4v**, M1 between dm-cu and wing margin/M1 between r-m and dm-cu; 5x, **ac**, third costal section between R2+3 and R4+5/fourth costal section; **adf**, longest dorsal branch of arista/width of first flagellomere; **arb**, dorsal branches/ventral branches of arista; **avd**, longest ventral branch/longest dorsal branch of arista in length; **BL**, body length; **C**, second costal section between subcostal break and R2+3/third costal section between R2+3 and R4+5; **C3F**, length of heavy setation in third costal section/length of the third costal section **ch/o**, maximum width of gena/maximum diameter of eye; **CuA1** between dm-cu and wing margin/dm-cu between M1 and CuA1; **dcl**, anterior dorsocentral/posterior dorsocentral in length; **dcp**, length distance between ipsilateral dorsocentrals/cross distance between anterior dorsocentrals; **flw**, length/width of first flagellomere; **FW/HW**, frontal width/head width; **M**, CuA1 between dm-cu and wing margin/M1 between r-m and dm-cu; **orbito**, distance between proclinate and posterior reclinate orbitals/distance between inner vertical and posterior reclinate orbital; **presctl**, prescutellar/posterior dorsocentral in length; **prorb**, proclinate orbital/posterior reclinate orbital in length; **rcorb**, anterior reclinate orbital/posterior reclinate orbital in length; **sctl**, basal scutellar/apical scutellar in length; **sctlp**,

distance between ipsilateral scutellars/cross distance between apical scutellars; **sterno**, anterior katepisternal/posterior katepisternal in length; **THL**, thorax length; **vb**, subvibrissal/vibrissa in length; **WL**, wing length; **WW**, wing width.

DNA Extraction and Sequencing

Total DNA was extracted using a DNA extraction Kit (TIANGEN, www.tiangen.com) according to the manufacturer's protocol. The *ND2* and *COI* fragments were amplified with the primers listed in Table 2. The PCR reactions consisted of an initial 4 min pre-denaturation at 94°C, followed by 30 cycles (30 sec of denaturation at 94°C, 1 min of annealing at 54°C for *ND2* and at 49°C for *COI*, and 1 min of extension at 72°C), and a final elongation for 5 min at 72°C. When possible, purified amplified products were directly run on an ABI 3730 sequencer; otherwise, they were cloned into the pMD18-T vector (TAKARA, www.takara-bio.com) and then sequenced. The related *ND2* sequences of *A. natagai*, *A. planate*, and *A. sinuata* were retrieved from the National Center for Biotechnology Information (NCBI).

Phylogenetic analyses

The sequences were aligned by the Clustal W (Thompson et al. 1994) method in MEGA 4.0 (Tamura et al. 2007) with the default options and then adjusted manually. Because the substitution saturation masked the phylogenetic signal (Lopez et al. 1999; Philippe and Froterre 1999), the method of Xia et al. (2003) was used to test the nucleotide substitution saturation in the program DAMBE 5.0.80 (Xia and Xie 2001). The base compositions of these sequences were investigated using PAUP* version 4.0b10 (Swofford 2001), and the c^2 test was used to evaluate the nucleotide composition

homogeneity among them. Uncorrected *p* distance among taxa was estimated by MEGA 4.0 (Tamura et al. 2007).

Phylogenetic relationships were constructed using the Bayesian inferring (BI) method in MrBayes 3.2.1 (Huelsenbeck and Ronquist 2001; Ronquist and Huelsenbeck 2003). In the BI analyses, the data were partitioned by locus (1 data partition) and codon positions (3 data partitions). The nucleotide substitution models of BI analyses were selected by Modeltest 3.7 using the hierarchical likelihood ratio test (hLRT) criterion (Posada and Crandall 1998). Two independent runs with 2,000,000 generations were implemented in parallel, and a sampling frequency of every 100 generations was employed. When the average deviation of split frequencies fell well below 0.01, the two runs were stopped. For each run, the 5,000 early-phase samples were discarded, and the remainder of the samples were used. A majority rule tree showing all the compatible partitions was obtained.

Nomenclature
This publication and the nomenclature it contains have been registered in ZooBank. The LSID number is: urn:lsid:zoobank.org:pub:60353BF6-3506-4286-A8E9-FB72847CD3D9. It can be found online by inserting the LSID number after www.zoobank.org/.

Results

Amiota taurusata species group

Diagnosis
Hind femur with small, lobe-like flap baso-ventrally; fourth tergite laterally broadened and protruded more than others (modified from Chen and Toda 2001; Figures 1B, 2D).

In the new species described, only characters that depart from the universal description (given by Chen and Toda (2001) and Chen et al. (2004, 2005) for the subgenus *Amiota*) are provided for brevity.

Amiota protuberantis Shao et Chen, sp. nov.
(Figure 1)

Diagnosis
This species very similar to *A. femorata* Chen et Takamori, 2005 in hind tibia distinctly expanded on subapical part of dorsal surface; aedeagus bifurcated on basal 1/2, submedially slightly curved dorsad, separated from parameres in lateral view (Figure 1D).

Description
Only important characters are given. Male and female: Frons, face, and clypeus nearly black. Ventral branches of arista distinctly shorter than 1/3 of dorsals in male, slightly shorter than 1/2 of dorsals in female. Palpus brown. Legs yellow except for dark brown on all femora in female or dark brown on femora of fore- and midlegs and distal half of hind femur in male. Male hindleg apico-dorsally much extended like flap on tibia and dorsally slightly expanded on first tarsomere. Epandrium small, constricted more than 1/2 width mid-dorsally, with ca. 17 setae near posterior to ventral margins on each side (Figure 1A). Surstylus distally with numerous setae on outer surface and ca. 7 prensisetae (Figure 1B). Vertical lobe of gonopod apically round, without any processes. Parameres fused on basal 3/4, slightly sclerotized, as long as aedeagus, with ca. 9 sensilla subbasally (Figure 1C, D).

Measurements
BL = 3.08 mm in the holotype (range in 3 ♂ and 2 ♀ paratypes: 2.60–3.16 mm in ♂, 3.32–3.40 mm in ♀), THL = 1.76 mm (1.56–1.72
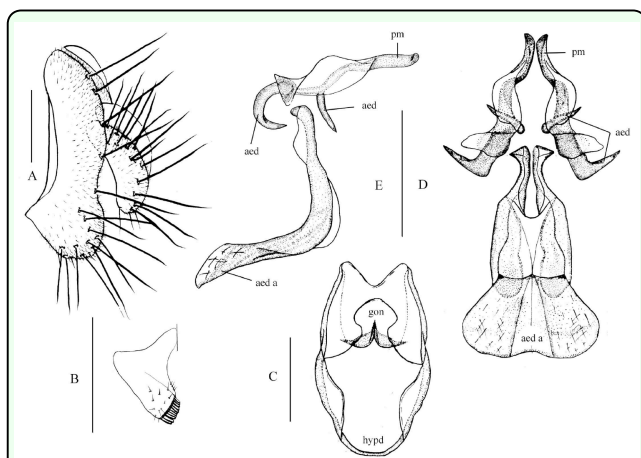
Figure 2. *Amiota shennongi* Shao et Chen, **sp. nov.** ♂: (A) Epandrium (epand) and circus, lateral view; (B) surstylus (sur) and tenth sternite (st 10), ventral view; (C) hypandrium and gonopod, ventral view; (D, E) paramere(s), aedeagus, and aede-agal apodeme, ventral and lateral views. Scale bars: 0.1 mm. High quality figures are available online.

mm in ♂, 1.60–1.64 mm in ♀), WL = 2.60 mm (2.24–2.60 mm in ♂, 2.80–2.88 mm in ♀), WW = 1.20 mm (1.00–1.20 mm in ♂, 1.20–1.32 mm in ♀, arb = 6/4 (6/4–5), avd = 0.33 (0.33–0.57), adf = 1.00 (0.88–1.17), flw = 1.83 (1.50–2.00), FW/HW = 0.39 (0.36–0.44), ch/o = 0.08 (0.08–0.10), prorb = 0.94 (0.69–1.00), rcorb = 0.50 (0.50–0.85), vb = 0.57 (0.57–0.63), dc1 = damaged, presct1 = 0.44 (0.44–0.60), sct1 = 1.20 (1.20–1.26), sterno = 0.78 (0.60–0.95), orbito = 1.00 (1.00–1.40), dcp = 0.38 (0.30–0.41), sct1p = 0.92 (0.72–1.33), C = 2.05 (1.83–3.08), 4c = 1.73 (0.93–1.78), 4v = 3.00 (2.50–3.00), 5x = 1.33 (1.16–2.00), ac = 3.25 (3.25–5.33), M = 0.64 (0.50–0.77), and C3F = 0.78 (0.78–0.83).

Types
Holotype ♂ (SCAU, No. 121088), CHINA: Mt. Wuliang, Jingdong, Yunnan, 18°41'N, 108°52'E, altitude 2200 m a.s.l., 4.viii.2006, T Li. Paratypes: 3 ♂, 2 ♀ (SCAU, No. 121089–93), same data as the holotype.

Etymology
From the Latin word protuberantis, referring to the hindleg tibia expanded on subapical part of dorsoposterior surface.

Distribution
China (Yunnan).

***Amiota shennongi* Shao et Chen, sp. nov.**
(Figure 2)

Diagnosis
This species very similar to *A. aquilotaurusata* Takada, Beppu et Toda, 1979 in that it has the same shape of the male terminalia. It differs by having the short process of aedeagus longer than 1/2 of long one (Figure 2D, E), the paramere thick rod-like, not expanded (Figure 1D, E).

Description
Only important characters are given in here. Male: Frons, face, and clypeus nearly dark brown. Ventral branches of arista distinctly shorter than 1/3 of dorsals in male. Palpus brownish yellow. Legs entirely yellow; hind leg: tibia apico-dorsally much extended flap, and first tarsomere dorsally expanded (Chen and Toda 2001; Figure 2D). Epandrium entirely separated into two lateral lobes, with about 15 setae near posterior to ventral margins per site (Figure 2A). Surstylus lacking pubescence, with finger-like process at posteroventral corner, and about nine prensisetae on distal margin (Figure 2B). Tenth sternite deeply constricted mid-ventrally, but not separated, entirely fused to surstyli laterally (Figure 2B). Anterior portion of hypandrium slightly broadened (Figure 2C). Aedeagus basally fused to paramere and deeply bifurcated, two processes of aedeagus nearly equilong (Figure 2D, E). Parameres

slightly longer than aedeagus, round apically and expanded basally (Figure 2D, E).

Measurements
BL = 2.88 mm in the holotype (3.00 mm in 1♂ paratype), THL = 1.16 mm (1.27 mm), WL = 2.14 mm (2.44 mm), WW = 0.96 mm (1.24 mm), arb = 7/5 (5/4), avd = 0.29 (0.33), adf = 1.40 (1.20), flw = 2.40 (2.00), FW/HW = 0.46 (0.38), ch/o = 0.34 (0.24), prorb = 1.08 (0.87), rcorb = 0.75 (0.66), vb = 0.43 (0.50), dc1 = damaged (0.6), presct1 = 0.28(0.50), sct1 = 1.23 (1.09), sterno = 1.50 (0.75), orbito = 1.40 (3.30), dcp = 0.32 (0.36), sct1p = 1.33 (1.33), C = 2.57 (1.67), 4c = 1.27 (2.10), 4v = 3.55 (3.40), 5x = 0.63 (0.75), ac = 3.50 (5.25), M = 0.80 (0.80), and C3F = 0.63 (0.59).

Types
Holotype ♂ (SCAU, No. 121094), CHINA: Dajiuhu, Shennongjia, Hubei, 31°29'N, 110°18'E, altitude 1400 m a.s.l., 31.vii.2004, HW Chen. Paratype: 1♂ (SCAU, No. 121095), same data as holotype.

Etymology
Patronym, the name of Yandi, who was a man in an old Chinese story.

Distribution
China (Hubei).

Key to species of the *taurusata* group
1. Hind femur ventro-basally with nearly hyaline, small, lobe-like flap; fourth tergite laterally broadened and protruded more than others (the *taurusata* group).………………………………………......2
  – Hind femur without any flap; fourth tergite neither broadened nor protruded more than others…..............other *Amiota* species

2. Ventral branches of arista distinctly shorter than 1/2 of dorsals; all femora dark brown to black……………………….…..…….3
  – Ventral branches of arista as long as 1/2 of dorsals; all legs yellow…........................5

3. Hind first tarsomere not expanded dorsally………………………………….4
  – Hind first tarsomere expanded dorsally………..*A. sacculipes* Máca et Lin

4. Vertical lobe of gonopod nearly triangular; aedeagus basally with 1 pair of slender processes…*A. femorata* Chen et Takamori
  – Vertical lobe of gonopod nearly quadrate; aedeagus without any processes…………. …..*A. protuberantis* Shao et Chen, sp. nov.

5. Hind tibia apicodorsally much extended like flap; hind first tarsomere expanded dorsally…..6
  – Hind tibia apicodorsally not extended like flap; hind first tarsomere not expanded dorsally…………………………………8

6. Short process of aedeagus shorter than 1/5 of long one……………………………….. ……..*A. taurusata* Takada, Beppu et Toda
  – Short process of aedeagus slightly shorter or longer than 1/2 of long one..………..........7

7. Short process of aedeagus shorter than 1/2 of long one; paramere expanded to lobe-like…..*A. shennongi* Shao et Chen, sp. nov.
  – Short process of aedeagus longer than 1/2 of long one; paramere expanded to lobe-like...….........*A. aquilotaurusata* Takada, Beppu et Toda

8. Parameres nearly entirely sclerotized; gonopod nearly triangular……………….... ………....*A. asymmetrica* Chen et Takamori
  – Parameres with membranaceous part; gonopod nearly quadrate………………...9

9. Paramere entirely separated from aedeagus..
...............*A. yixiangna* Chen et Takamori
– Paramere basally fused to aedeagus...........
..............*A. vulnerabla* Chen et Zhang
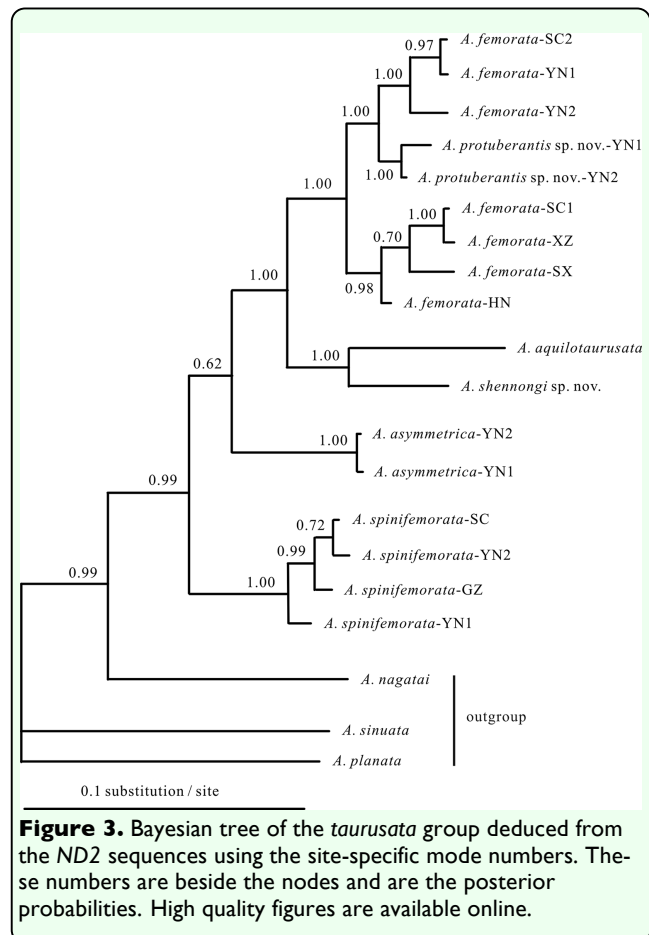
Molecular analysis

Data set analysis
The alignment of the sequences included 1026 base pairs for *ND2* and 684 for *COI*. There were end gaps in the *ND2* sequences of *A. spinifemorata* –GZ (sites 1–36), *A. spinifemorata* –YN2 (sites 1015–1026), and *A. shennongi* **sp. nov**. (sites 1015–1026). End gaps also existed in the *ND2* sequences (sites 149–151) of *A. femorata* –HN, *A. femorata* –SC2, *A. femorata* –SX, *A. femorata* –YN2, and *A. protuberantis* **sp. nov**.–YN2 as well as in the *ND2* sequences (sites 148–150) of *A. femorata* –SC1, *A. femorata* –YN2, *A. femorata* –XZ, and *A. protuberantis* **sp. nov**.–YN2. The *COI* sequences of some samples (*A. aquilotaurusata*, *A. asymmetrica* –YN2, and *A. femorata* –HN) were not acquired, and end gaps existed in the *COI* sequences (sites 1–15) of *A. plannata*. There were 349 variable sites (of which 211 were parsimony informative sites) for *ND2* and 178 variable sites (of which 106 were parsimony informative sites) for *COI*. The nucleotide composition of *ND2* is shown in Table 3. The sequences contained much higher AT content (82.8%) than GC content, especially at the third codon positions (95.4%). The c^2 test revealed that the nucleotide composition among the taxa was not hetheterogeneous.

Regardless of whether the analysis was performed with the combined or separated codon position data for *ND2*, the test of substitution saturation revealed that the observed substitution saturation index (*Iss*) was significantly lower than the corresponding critical substitution saturation index (*Iss.c*) for both the symmetrical and asymmetrical trees, indicating that there was little saturation in these sequences (Table 4).

Table 5 shows the uncorrected pairwise divergence for the *ND2* and *COI* sequences in the *taurusata* group, excluding the p-distance for *COI* of *A. aquilotaurusata*, *A. asymmetrica* –YN1, and *A. femorata* –HN. The interspecific genetic divergence for *ND2* in the *taurusata* group ranged from 0.0294 (*A. femorata* vs. *A. protuberantis* **sp. nov.**) to 0.1049 (*A. aquilotaurusata* vs. *A. spinifemorata*), and for *CO1* it ranged from 0.0207 (*A. femorata* vs. *A. protuberantis* **sp. nov.**) to 0.0841 (*A. asymmetrica* vs. *A. protuberantis* **sp. nov.**). The intraspecific genetic divergences for *ND2* and *COI* were calculated for *A. asymmetrica* (0.0021 for *ND2*), *A. protuberantis* **sp. nov.** (0.0072 for

Figure 3. Bayesian tree of the *taurusata* group deduced from the *ND2* sequences using the site-specific mode numbers. These numbers are beside the nodes and are the posterior probabilities. High quality figures are available online.

ND2, 0.0015 for *COI*), *A. spinifemorata* (0.0041 to 0.0185 for *ND2*, 0.0073 to 0.0088 for *COI*), and *A. femorata* (0.0010 to 0.0474 for *ND2*, 0.0000 to 0.0336 for *COI*).

Phylogenetic analysis

The Bayesian tree for *ND2* lent good support for the monophyly of the *taurusata* group with respect to the outgroups (posterior probabilities (PP) = 0.99) (Figure 3). Samples from different geographical areas of *A. protuberantis*, *A. asymmetrica*, and *A. spinifemorata* clustered as a monophyletic lineage, while samples of *A. femorata* were rendered paraphyletic with respect to *A. protuberantis*. *A. spinifemorata* first diverged in the *taurusata* group and was then followed by *A. asymmetrica*. The other four species grouped into a robust supported group (PP = 1.00). *A. shennongi* **sp. nov.** and *A. aquilotaurusata* showed a sibling relationship (PP = 1.00) in agreement with their high similarity in morphological characters. Samples of *A. femorata* diverged into two highly supported clusters. One consisted of *A. femorata* (HN, SC1, SX, and XZ) (PP = 0.98); the other consisted of *A. femorata* (SC2 and YN1–2) (PP = 1.00) and clustered with *A. protuberantis* **sp. nov.** (PP = 1.00).

Discussion

A phylogenetic tree of the *taurusata* group was constructed using mitochondrial *ND2* sequences. As negative results were obtained in the tests of nucleotide composition heterogeneity and substitution saturation, the conclusions of the phylogenetic analyses should be accepted. The monophyly of the *taurusata* group was strongly supported in molecular phylogenetic analyses, and the relationships within this group were almost resolved. However, the unstable position of *A. asymmetrica and A. spinifemorata* was not

resolved, even when using a site-specific model for Bayesian inference. To fully resolve the phylogenetic relationship in the *taurusata* group, multiple loci or more species in the analyses are necessary.

The *ND2* divergence matrix was provided for the *taurusata* group. The interspecific genetic divergence in the *taurusata* group ranged from 0.0294 to 0.1049, and the intraspecific genetic divergence ranged from 0.0010 to 0.0474. The geographical samples of *A. asymmetrica*, *A. protuberantis* **sp. nov.**, and *A. spinifemorata* formed highly-supported monophyletic groups in the phylogenetic tree, and intraspecific genetic divergence within them was much less than interspecific genetic divergence in the *taurusata* group. In addition, no diagnostic morphological character was found to distinguish the geographical samples of these species, indicating that they should be considered conspecific. However, *A. femorata* diverged into two clusters, and classified characters in its morphology were missing. The three haplotypes of *A. femorata*, i.e., SC2, YN1, and YN2, clustered with *A. protuberantis* **sp. nov.** This relationship could be attributed to stochastic lineage sorting and/or hybridization. The genetic divergence for *ND2* within the two clusters ranged from 0.0010 to 0.0474, and the mean divergence between them was 0.0392. Assuming the observed divergence range (0.0294 to 0.1049) reflects the real intraspecific variations in the *taurusata* group, there likely are cryptic species in *A. femorata* samples.

Recent work suggests that cytochrome c oxidase I (*COI*) might serve as a DNA barcode for the identification of animal species (Brown et al. 2003; Foster et al. 2004; Barrett and Hebert 2005; Cardoso and Vogler 2005; Hogg and Hebert 2005; Monaghan et al. 2005; Vences et al. 2005; Ward et al. 2005).

This gene region is easily recovered and provides good resolution, as evidenced by the deep sequence divergences among 13,000 closely related pairs of animal species (Hebert et al. 2003b). In this study, a 684 bp region of *COI* was acquired, and it showed that *COI* differences between most of the species far exceeded those within species. The interspecific genetic divergence in the *taurusata* group ranged from 0.0207 to 0.0841, and the intraspecific genetic divergence ranged from 0.0000 to 0.0336. An overlapping area existed between the intraspecific and interspecific genetic divergence. The intraspecific genetic divergences within *A. protuberantis* **sp. nov.** (0.0015) and *A. spinifemorata* (0.0073 to 0.0088) were much lower than the minimum interspecific genetic divergence (0.0207) and the mean intraspecific variability for Diptera (1.3 ± 1.6%) (Meier 2008), indicating that they should be considered conspecific. This result is consistent with the *ND2* result and the morphology analysis. The observed divergence of the two clusters of *A. femorata* was 0.0322, which is greater than the minimum interspecific genetic divergence but lower than the minimum interspecific genetic divergence for Diptera (5.9 ± 4.1%) (Meier 2008). *A. protuberantis* **sp. nov.** was identified as the sister-species of *A. femorata*, and the p-distance ranged from 0.0146 to 0.0263. Because of the limit coming from the number and distribution of samples, there likely are cryptic species in the two clusters, which is consistent with the *ND2* result. It is important to include samples from a wider geographical range in future studies to determine if the two clusters represent morphologically cryptic species. Further samples are also needed for an evaluation of the morphological variability revealed in the results.

Biogeographical implications

All the members of *A. spinifemorata* and *A. asymmetrica* were found in southwestern China. According to the phylogenetic analyses, the two species diverged from the *taurusata* group prior to *A. shennongi* **sp. nov.** and *A. aquilotaurusata*, which were found in central and northeast China. It may indicate that the founder of the *taurusata* group arose in southwestern China, undergoing some differentiation before the expansion into the central and northern areas. In the zones of low and high elevation, *A. femorata* can be distributed between one cluster (*A. femorata* –HN, SC1, SX, excluding *A. femorata* –XZ) mainly at low elevations (ca. 300–500 m a.s.l.) and another cluster (*A. femorata* –SC2, YN1, and YN2) at high elevations (ca. 1700–2700 m a.s.l.) that clusters with *A. protuberantis* **sp. nov.** This result may indicate that some individuals underwent heteromorphosis to different extents following the expansion of *A. femorata* from low elevations into high elevations, and that then *A. protuberantis* **sp. nov.** was found.

Acknowledgements

References

Barrett RDH, Hebert PDN. 2005. Identifying spiders through DNA barcodes. *Canadian Journal of Zoology* 83: 481–491.

Brown JW, Miller SE, Horak M. 2003. Studies on New Guinea moths. 2. Description of a new species of *Xenothictis meyrick* (Lepidoptera: Tortricidae: Archipini).

Proceedings of the Entomological Society of Washington 105: 1043–1050.

Cao HL, Li T, Zhang WX, Chen HE. 2008. Five new species and five new records of the genus *Amiota* Loew (Diptera: Drosophilidae) from Hengduan Mountains, southwestern China. *Oriental Insects* 42: 193–205.

Cao H, Wang X, Gao J, Prigent SR, Watabe H, Zhang Y, Chen H. 2011. Phylogeny of the African and Asian *Phortica* (Drosophilidae) deduced from nuclear and mitochondrial DNA sequences. *Molecular Phylogenetics and Evolution* 61: 677–685.

Cardoso A, Vogler AP. 2005. DNA taxonomy, phylogeny and Pleistocene diversification of the *Cicindela hybrida* species group (Coleoptera: Cicindelidae). *Molecular Ecology* 14: 3531–3546.

Chen HW, Toda MJ. 2001. A revision of the Asian and European species in the subgenus *Amiota* Loew (Diptera, Drosophilidae) and establishment of species-groups based on phylogenetic analysis. *Journal of Natural History* 35: 1571–1563.

Chen HW, Watabe H, Gao JJ, Takamori H, Zhang YP, Aotsuka T. 2005. Species diversity of the subgenus *Amiota* (s. str.) Loew, 1862 (Diptera, Drosophilidae) in southern China. *Journal of Natural History* 39: 265–310.

Chen HW, Zhang CT, Liu GC. 2004. New species and new records of the subgenus *Amiota* s. str. Loew (Diptera, Drosophilidae) from North America, East Asia and Oceania. *Annales de la Société entomologique de France* 40: 59–67.

Favret C, Voegtlin DJ. 2004. Speciation by host-switching in pinyon *Ciniara* (Insecta : Hemiptera : Aphididae). *Molecular Phylogenetics and Evolution* 32: 139–151.

He XF, Jiang JJ, Cao HZ, Chen HW. 2009a. Taxonomy and molecular phylogeny of the *Amiota nagatai* species group (Diptera, Drosophilidae). *Zootaxa* 2193: 53–61.

He XF, Gao JJ, Cao HZ, Zhang XL, Chen HW. 2009b. Taxonomy and molecular phylogeny of the *Phortica hani* species complex (Diptera, Drosophilidae). *Zoological Journal of the Linnean Society* 157: 359–372.

Hogg ID, Hebert PDN. 2004. Biological identification of springtails (Hexapoda: Collembola) from the Canadian Arctic, using mitochondrial DNA barcodes. *Canadian Journal of Zoology* 82: 749–754.

Huelsenbeck JP, Ronquist FR. 2001. MRBAYES: Bayesian inference of phylogenetic trees. *Bioinformatics* 17: 754–755.

Li T, Cao HZ, Gao JJ, Chen HW. 2010. A revision of the subgenus *Stegana* (s. str.) (Diptera, Drosophilidae) from mainland China. *Zoological Journal of the Linnean Society* 158: 726–739.

Lu JM, Gao J J, Chen, XP, Chen HW. 2011a. The *Stegana undulata* species group (Diptera, Drosophilidae), with molecular phylogenetic analysis of the Chinese species. *European Journal of Entomology* 108: 139–152.

Lu JM, Li T, Chen HW. 2011b. Molecular phylogenetic analysis of the *Stegana ornatipes* species group (Diptera: Drosophilidae) in China, with description of a new species. *Journal of Insect Science*, 11:20. Available online: www.insectscience.org/11.20

Lopez P, Forterre P, Philippe H. 1999. The root of the tree of life in the light of the covarion model. *Journal Molecular Evolution* 49: 496–508.

Meier R, Zhang G, Ali F. 2008. The use of mean instead of smallest interspecific distances exaggerates the size of the "Barcoding Gap" and leads to misidentification. *Systematic Biology* 57: 809–813.

Park J. 1999. *Molecular phylogenetic studies of the Drosophila (Drosophila) virilis section (Diptera, Drosophilidae)*. PhD. Thesis, Tokyo Metropolitan University.

Philippe H, Forterre P. 1999. The rooting of the universal tree of life is not reliable. *Journal Molecular Evolution* 49: 509–523.

Posada D, Crandall KA. 1998. Modeltest: testing the model of DNA substitution. *Bioinformatics* 14: 817–818.

Ronquist F, Huelsenbeck JP. 2003. MrBayes 3: Bayesian phylogenetic inference under mixed models. *Bioinformatics* 19: 1572–1574.

Swofford DL. 2001. *PAUP*[*]: *Phylogenetic analysis using parsimony ([*] and other methods)*, version 4.0. Sinauer.

Tamura K, Dudley J, Nei M, Kumar S. 2007. MEGA4: Molecular Evolutionary Genetics Analysis (MEGA) software version 4.0. *Molecular Biology and Evolution* 24: 1596–1599.

Thompson JD, Higgins DG, Gibson TJ. 1994. Clustal W: improving the sensitivity of progressive multiple sequence alignment through sequence weighting, position specific gap penalties and weight matrix choice.

Nucleic Acids Research 22: 4673–4680.

Xia XH, Xie ZH. 2001. DAMBE: Data analysis in molecular biology and evolution. *Journal of Heredity* 92: 371–373.

Vences M, Thomas M, van der Meijden A, Chiari Y, Vieites DR. 2005. Comparative performance of the 16S rRNA gene in DNA barcoding of amphibians. *Frontiers in Zoology* 2: 1–12.

Ward RD, Zemlak TS, Innes BH, Last PR, Hebert PDN. 2005. DNA barcoding Australia's fish species. *Philosophical Transactions Of The Royal Society B: Biological Sciences* 360: 1847–1857.

Xia XH, Xie ZH, Salemi M, Chen L, Wang Y. 2003. An index of substitution saturation and its application. *Molecular Phylogenetics and Evolution* 26: 1–7.

Zhang WX, Toda MJ. 1992. A new species-subgroup of the *Drosophila immigrans* species-group (Diptera, Drosophilidae), with description of two new species from China and Revision of Taxonomic Terminology. *Japan Journal Entomology* 60: 839–850.

Zhao F, Gao JJ, Chen HW. 2009. Taxonomy and Molecular Phylogeny of the Asian Paraleucophenga Hendel (Diptera, Drosophilidae). *Zoological Journal of the Linnean Society* 155: 615–629.

Table 1. Data on samples for DNA sequencing and the accession numbers of the *ND2* and *COI* sequences.

Species groups	Species	Collection locality in China	Altitude	Latitude and longitude	Accession numbers of *ND2*	Accession numbers of *COI*
apodemata	*plannata*	Fusui, Guangxi	200 m	22°41'N, 107°32'E	EU431849[1]	JQ676819
nagatai	*nagatai*	Guangzhou, Guangdong	300 m	24°50'N, 123°52'E	FJ360718[1]	JQ676820
sinuata	*sinuata*	Ledon, Hainan	200 m	18°41'N, 108°52'E	EU431843[2]	JQ676821
taurusata	*aquilotaurusata*	Benxi, Liaoning	300 m	18°41'N, 108°52'E	EU431882	
	asymmetrica –YN1	Kunming, Yunnan	1900 m	25°02'N, 102°43'E	JN661375	
	asymmetrica –YN2	Weixi, Yunnan	1900 m	24°32' N, 101°01' E	EU431841	JQ676822
	femorata –HN	Shangzhi, Hunan	300 m	23°17'N, 113°33'E	JN661376	
	femorata –SC1	Baoxing, Sichuan	500 m	27°43'N, 117°57'E	JN661377	JQ676823
	femorata –SC2	Danba, Sichuan	2700 m	30°41'N, 101°45'E	EU431873	JQ676824
	femorata –SX	Foping, Shannxi	300 m	24°50'N, 123°52'E	JN661378	JQ676825
	femorata –XZ	Bomi, Xizang	2080 m	30°06'N, 95°05'E	JN661379	JQ676826
	femorata –YN1	Binchuan, Yunnan	1900 m	21°28'N, 101°38'E	JN661380	JQ676827
	femorata –YN2	Weixi, Yunnan	1700 m	21°28'N, 101°38'E	EU431915	JQ676828
	protuberantis –YN1	Jingdong, Yunnan	2200 m	18°41'N, 108°52'E	EU431872	JQ676829
	protuberantis –YN2	Jingdong, Yunnan	2400 m	18°41'N, 108°52'E	JN661381	JQ676830
	shennongi	Shennongjia, Hubei	1400 m	31°29'N, 110°18'E	JN661382	JQ676831
	spinifemorata –GZ	Xingyi, Guizhou	1400 m	24°59'N, 105°36'E	JN661383	JQ676832
	spinifemorata –SC	Emeishan, Sichuan	1700 m	30°10' N, 103°36' E	JN661384	JQ676833
	spinifemorata –YN1	Baoshan, Yunnan	1400 m	25°27'N, 98°52'E	JN661385	JQ676834
	spinifemorata –YN2	Binchuan, Yunnan	1900 m	25°27'N, 98°52'E	JN661386	JQ676835

[1]He et al. 2009a; [2]mistaken as EU431907 in He et al. 2009a.

Table 2. Primers used for PCR and sequencing.

Target gene	Primers	Primer sequence (5'-3')	Reference
ND2	H	AAGCTACTGGGTTCATACC	Park 1999
	T1	ATATTTACAGATTTGAAGG	Park 1999
	T3	AGGCGATAGATTGTAAATC	Li 2010
	T4	CTTTGAAGGCTATTAGTT	Present study
COI	LCO1490	GGTCAACAAATCATAAAGATATTGG	Folmer et al. 2010
	F1	CGCCTAAACTTCAGCCACTT	He et al. 2009a
	HCO2198	TAAACTTCAGGGTGACCAAAAAATCA	Folmer et al. 2010

Table 3. Results of nucleotide composition and composition homogeneity test.

ND-2 codon position	Nucleotide composition						Composition homogeneity test		
	T	C	A	G	A+T	C+G	X^2	df	*P*
All	47.3	9.9	35.5	7.3	82.8	17.2	4.7369	57	1
1st	43.6	8.2	37.3	10.9	80.9	19.1	5.8834	57	1
2nd	49.5	18.4	22.4	9.6	71.9	28	5.6731	57	1
3rd	48.7	3.2	46.7	1.4	95.4	4.6	16.153	57	1

Table 4. Results of substitution saturation tests and model selection.

ND2 codon position	Test of substitution saturation					Model
	Iss	*Iss.cSym*[a]	*PSym*[b]	*Iss.cAsym*[c]	*PAsym*[d]	
All	0.136	0.7568	0	0.5363	0	K81uf+I+G
1st	0.12	0.6912	0	0.4473	0	TIM+I+G
2nd	0.053	0.6912	0	0.4473	0	HKY+I+G
3rd	0.305	0.691	0	0.447	0	TrN+G

[a]Index of substitution saturation assuming a symmetrical true tree.
[b]Probability of a significant difference between *Iss* and *Iss.cSym* (two-tailed test).
[c]Index of substitution saturation assuming an asymmetrical true tree.
[d]Probability of a significant difference between *Iss* and *Iss.cAsym* (two-tailed test).

Table 5. Uncorrected pairwise p-distance among the *ND2* and *COI* sequences of the *taurusata* species group. The matrix in the lower left shows the uncorrected pairwise p-distance among the *ND2* sequences; the matrix in the upper right shows the uncorrected pairwise p-distance among the *COI* sequences.

Species	1	2	3	4	5	6	7	8	9	10	11	12	13	14	15	16	17	18	19	20
A. planata		0.1286	0.1211			0.1211		0.142	0.142	0.1405	0.142	0.1405	0.1405	0.1405	0.139	0.1256	0.1256	0.1271	0.1241	0.1286
A. nagatai	0.139		0.1111			0.1067		0.1053	0.1082	0.1038	0.1053	0.1067	0.1067	0.0994	0.0994	0.0994	0.098	0.0965	0.0994	0.0994
A. sinuate	0.1318	0.1462				0.1126		0.1199	0.1257	0.1184	0.1199	0.1243	0.1272	0.1184	0.117	0.1228	0.1155	0.1155	0.114	0.117
A. aquilotaurusata	0.1339	0.139	0.1483																	
A. asymmetrica-YN1	0.1246	0.1277	0.1236	0.104																
A. asymmetrica-YN2	0.1256	0.1277	0.1226	0.103	0.0021			0.0789	0.0833	0.0775	0.0789	0.0819	0.0833	0.0848	0.0833	0.0804	0.076	789	0.076	0.0789
A. femorata-HN	0.1329	0.138	0.1329	0.0968	0.0875	0.0886														
A. femorata-SC1	0.1339	0.1411	0.1359	0.0989	0.0896	0.0906	0.0082		0.0322	0.0015	0	0.0336	0.0322	0.0263	0.0249	0.0789	0.0775	0.0804	0.0804	0.0804
A. femorata-SC2	0.138	0.1401	0.1442	0.0999	0.0958	0.0968	0.033	0.034		0.0307	0.0322	0.0015	0.0058	0.0175	0.0161	0.0804	0.0833	0.0848	0.0863	0.0892
A. femorata-SX	0.1339	0.1421	0.1349	0.0989	0.0937	0.0947	0.0113	0.0134	0.0422		0.0015	0.0322	0.0307	0.0249	0.0789	0.0775	0.076	0.0789	0.0789	0.0789
A. femorata-XZ	0.1349	0.1421	0.137	0.0999	0.0906	0.0917	0.0093	0.001	0.035	0.0144		0.0336	0.0322	0.0263	0.0249	0.0789	0.0775	0.0804	0.0804	0.0804
A. femorata-YN1	0.137	0.139	0.1432	0.0989	0.0947	0.0958	0.033	0.034	0.0021	0.0402	0.035		0.0044	0.0161	0.0146	0.0789	0.0819	0.0833	0.0848	0.0877
A. femorata-YN2	0.1452	0.1483	0.1473	0.104	0.102	0.103	0.0381	0.0412	0.0134	0.0474	0.0422	0.0134		0.0175	0.0161	0.0775	0.0833	0.0848	0.0863	0.0892
A. protuberantis sp. nov.-YN1	0.1401	0.139	0.1421	0.0978	0.0958	0.0968	0.036	0.0371	0.0237	0.0433	0.0381	0.0237	0.0288		0.0015	0.0746	0.0746	0.076	0.0775	0.0804
A. protuberantis sp. nov.-YN2	0.137	0.137	0.137	0.0947	0.0927	0.0937	0.0288	0.0299	0.0165	0.036	0.0309	0.0165	0.0216	0.0072		0.0731	0.0746	0.076	0.0775	0.0804
A. shennongjia sp. nov	0.137	0.1339	0.1432	0.0649	0.102	0.1009	0.0834	0.0855	0.0886	0.0896	0.0865	0.0875	0.0978	0.0906	0.0886		0.0775	0.0789	0.0804	0.0775
A. spinifemorata-GZ	0.1298	0.1318	0.1318	0.105	0.0958	0.0947	0.0958	0.0989	0.1009	0.0989	0.0999	0.0999	0.104	0.105	0.102	0.0989		0.0073	0.0088	0.0088
A. spinifemorata-SC	0.1287	0.1308	0.1298	0.103	0.0927	0.0917	0.0927	0.0958	0.0999	0.0958	0.0968	0.0989	0.103	0.0999	0.0989	0.0968	0.0062		0.0073	0.0073
A. spinifemorata-YN1	0.1298	0.1298	0.1277	0.1009	0.0927	0.0917	0.0906	0.0937	0.0978	0.0937	0.0947	0.0968	0.103	0.0999	0.0968	0.0937	0.0165	0.0144		0.0088
A. spinifemorata-YN2	0.1267	0.1287	0.1298	0.1061	0.0947	0.0937	0.0927	0.0958	0.0999	0.0958	0.0968	0.0989	0.103	0.0999	0.0989	0.0968	0.0082	0.0041	0.0185	